## SUPPLEMENTARY FIGURES AND VIDEO

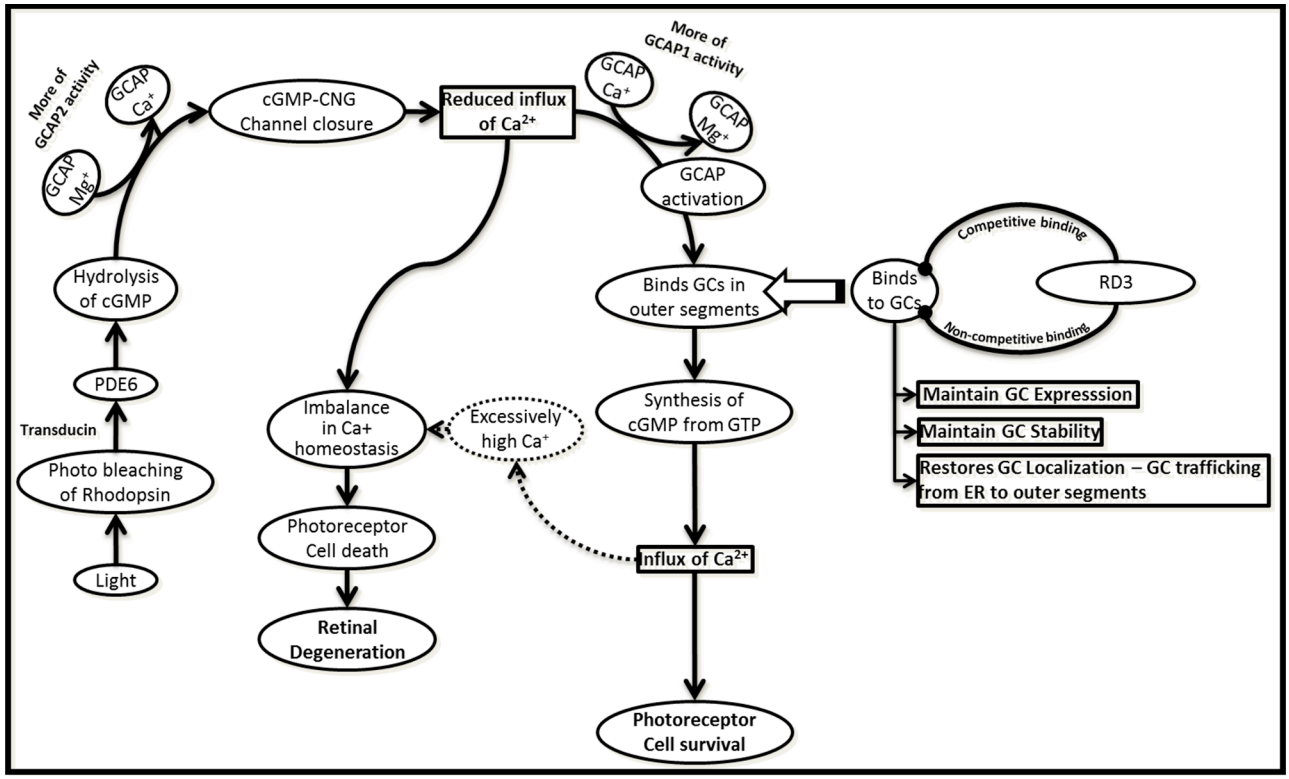


**Supplementary Figure S1: Schematic representation of the role of Retinal Degeneration Protein RD3 in photoreceptor cell survival.** Chart showing the mechanistic signal transduction flow through that affect photoreceptor cell survival and consequent retinal degeneration and, functional regulatory role of RD3 in this setting.

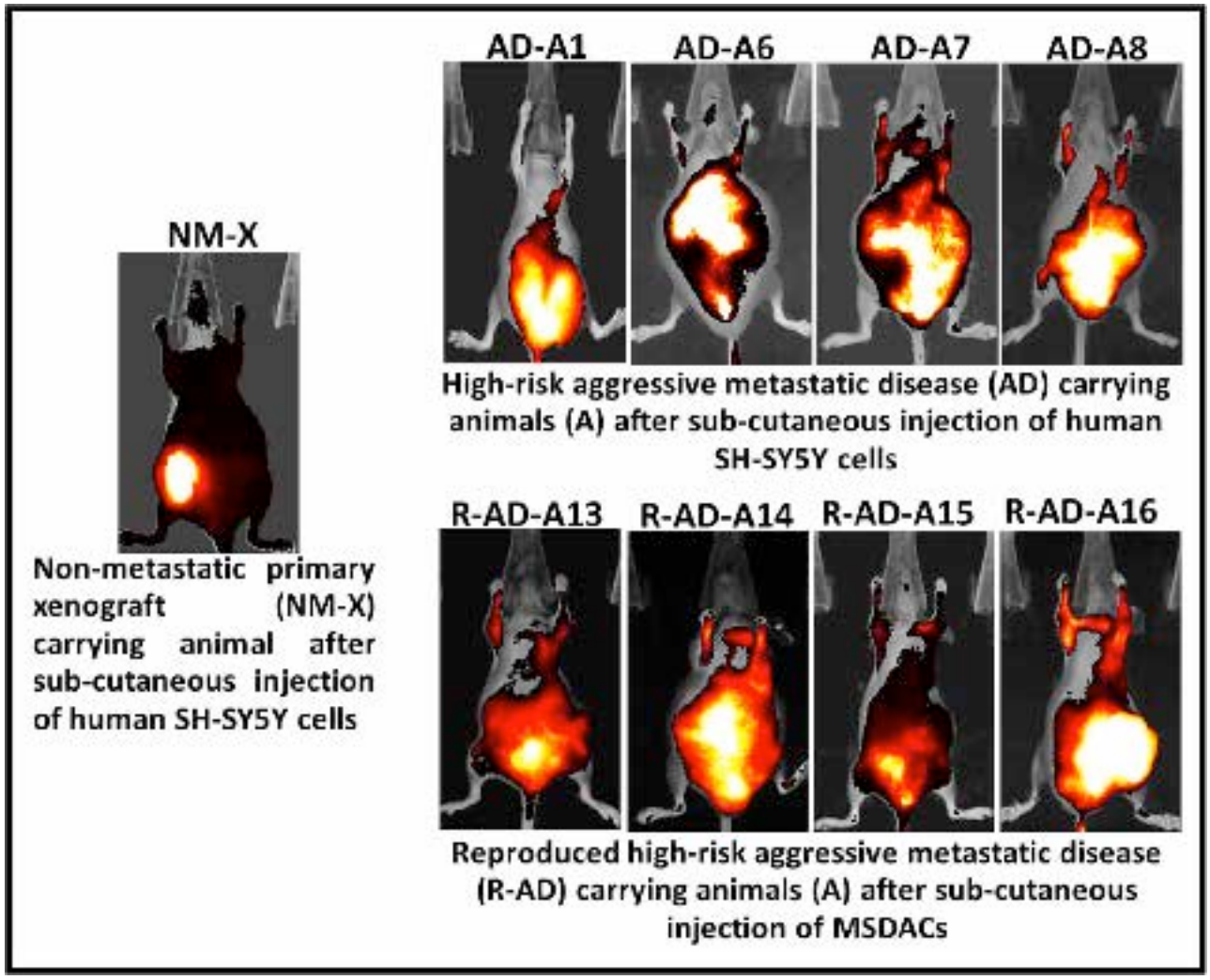


**Supplementary Figure S2: *In vivo* mouse model of reproducible high-risk aggressive metastatic neuroblastoma.** ***Left:*** *In vivo* fluorescent non-invasive tumor imaging showing neuroblastoma xenograft without any metastasis in animals that received sub-cutaneous injection of human SH-SY5Y cells in matrigel. ***Top Panel:*** *In vivo* fluorescent non-invasive tumor imaging showing the development of high-risk aggressive disease with tumor metastasis (in pelvic, retroperitoneal, abdominal and in chest cavities) in animals that received identical clones of SH-SY5Y cells under identical conditions. ***Bottom Panel:*** *In vivo* tumor imaging showing the reproducibility of high-risk aggressive disease with tumor metastasis (in pelvic, retroperitoneal, abdominal and in chest cavities) in animals that received metastatic site derived aggressive cells (MSDACs).

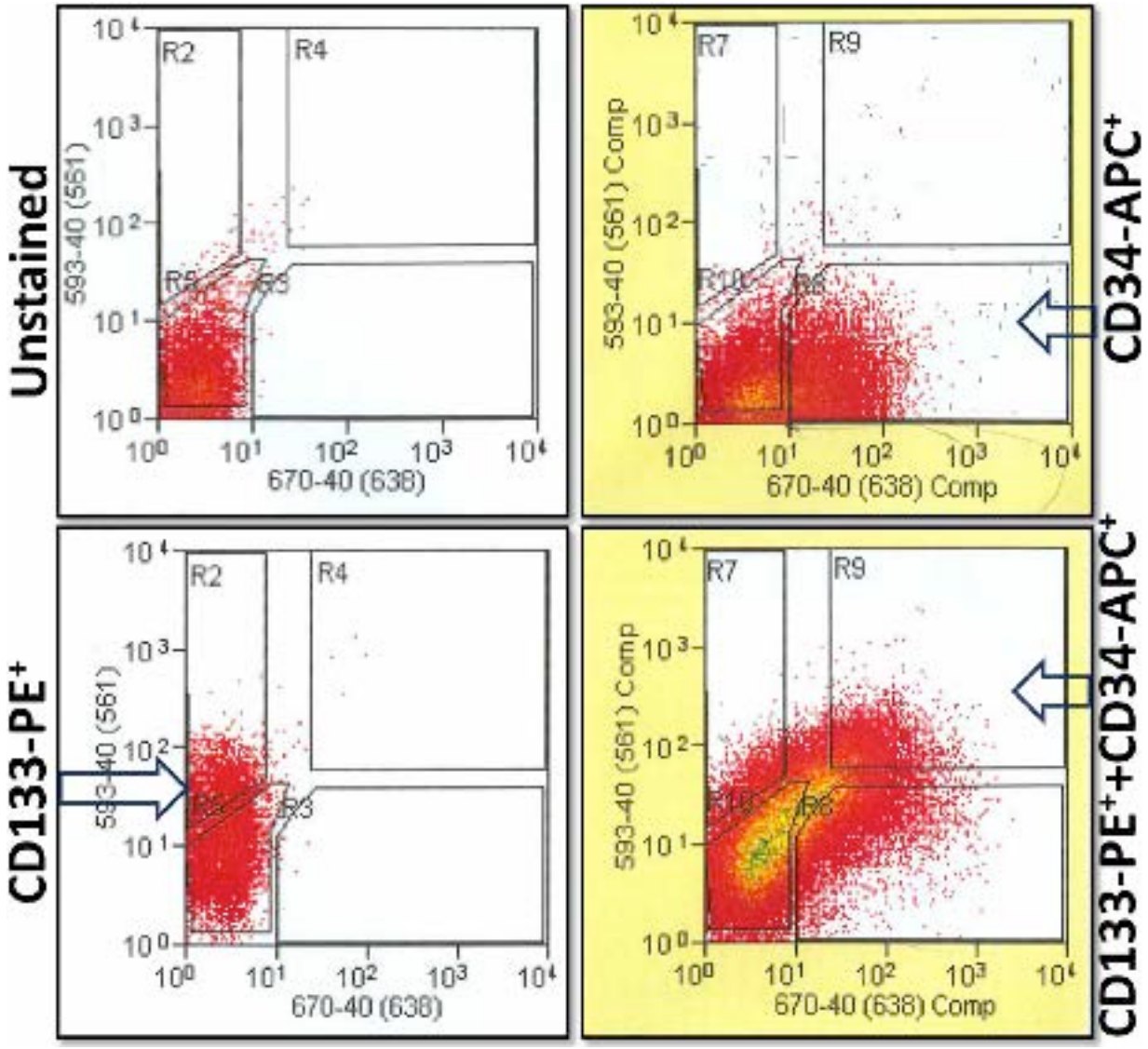


**Supplementary Figure S3: Flow-cytometry cell sorting of CD133$^+$+CD34$^+$ human NB CSCs.** Human CD133$^+$+CD34$^+$ neuroblastoma cells derived from non-metastatic xenografts or from the manifold of metastatic sites from different animals was sorted with the gate created based on the viable non-mouse derived cells (by excluding PI$^+$, mouse CD31$^+$, mouse lineage$^+$ or mouse H-2Kd$^+$), and the IgG2bk-APC (isotypic control for CD34-APC) and IgG2ak-PE (isotypic control for CD133-PE) antibodies.

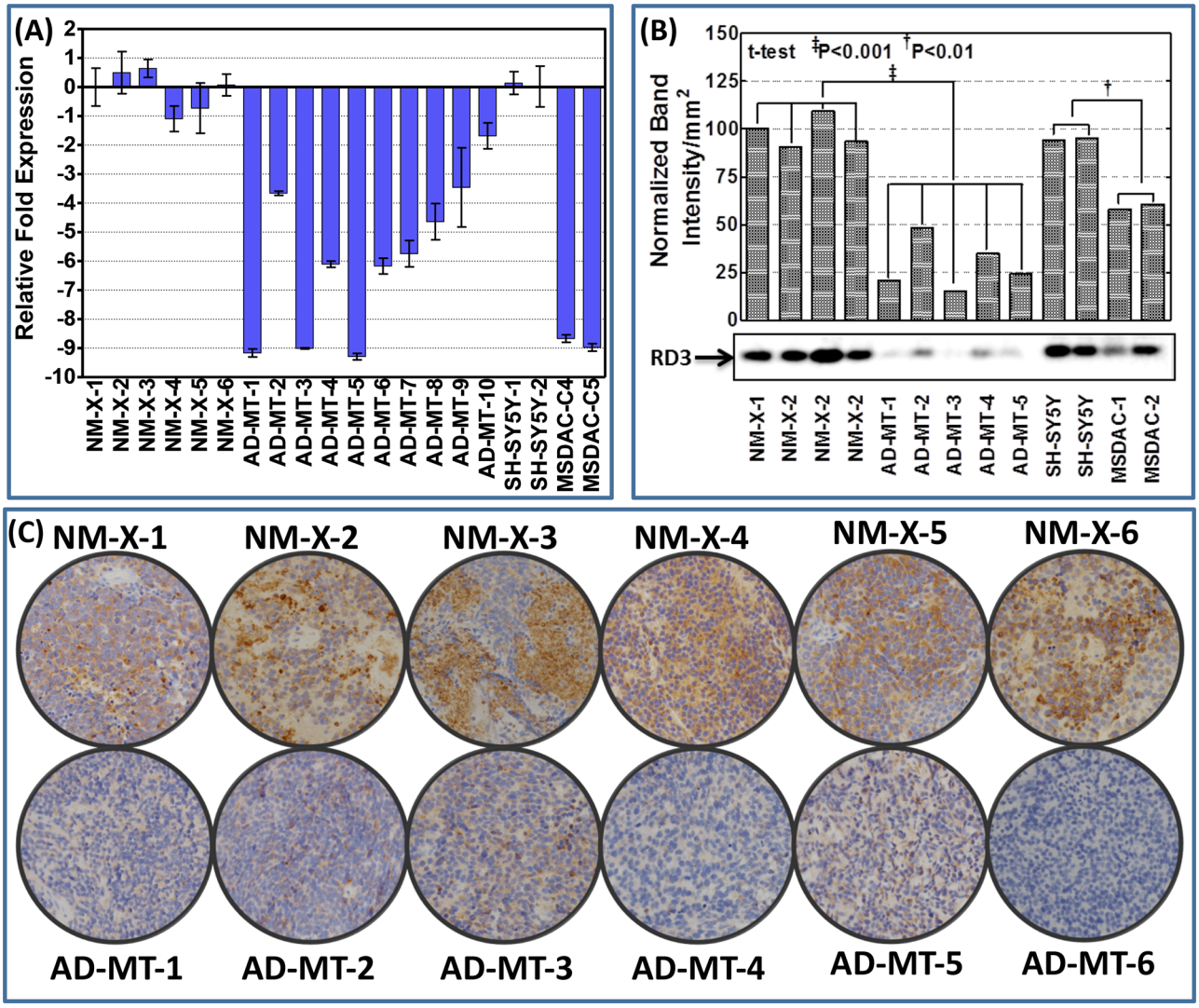


**Supplementary Figure S4: Loss of RD3 in high-risk aggressive neuroblastoma. A.** Histograms from QPCR analysis showing complete suppression of RD3-transcription in the manifold of tumor tissues from metastatic high-risk aggressive disease compared to the manifold of primary xenografts from the animals without aggressive disease and, in the clones of MSDACs cultured and maintained *ex vivo* compared to the clones of parental human SH-SY5Y cells. **B.** Representative immunoblots showing marked loss of RD3 in manifold of metastasized tumor tissues ($n = 5$) from aggressive disease bearing animals compared to the manifold of primary xenografts ($n = 4$) from animals that showed no aggressive disease. Densitometry analyses was performed using Quantity One Image analysis software and are compared using GraphPad PRISM software **C.** Representative photomicrographs (20X) showing RD3 localization and expression levels in a manifold of non-metastatic xenografts and, multifarious metastatic tumors. Automated RD3 IHC staining revealed strong and consistent positivity in non-metastatic xenografts and further demonstrated a complete loss of RD3 in metastasized tumors.

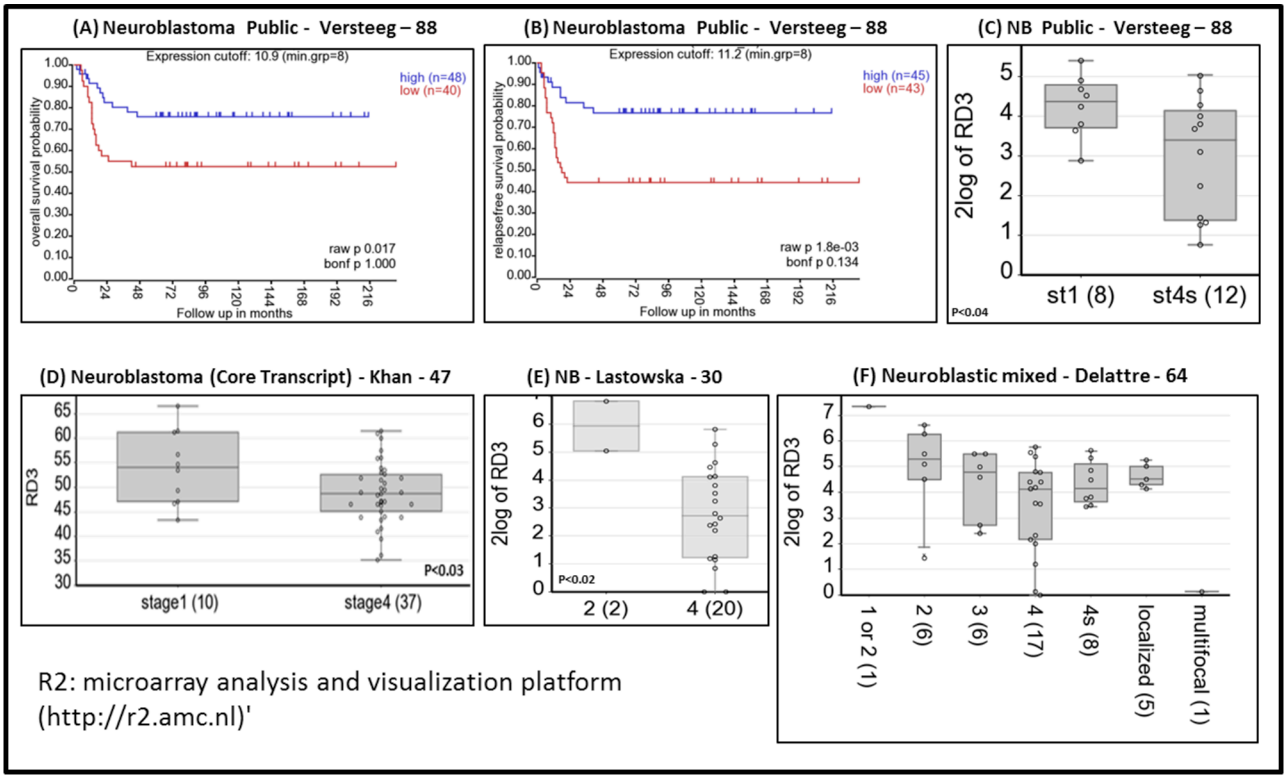


**Supplementary Figure S5: RD3 loss associates with poor clinical outcomes.** Correlation of RD3 expression with NB clinical outcomes in a cohort of 88 patients. **A.** Kaplan-Meier curve showing decreased OS in patients with low RD3 expression compared with high RD3 expression. **B.** Kaplan-Meier curve showing a pronounced decrease in relapse-free survival for patients with low RD3 expression. **C.** RD3 expression and disease progression: Box-whiskers plot with circles showing significant loss of RD3 in patients with high-risk 4S disease. **D.** Independent cohort of 47 patients showing significant decrease in RD3 expression between stage 1 and stage 4. **E.** Box-whiskers plot with circles showing complete loss of RD3 in high-risk aggressive metastatic stage 4 disease in a separate cohort of 30 patients. **F.** Graph showing stage-wise RD3 expression in a cohort of 64 patients. RD3 levels were high at stages 1 and 2. Levels decrease with disease progression and are significantly lower in multifocal disease.

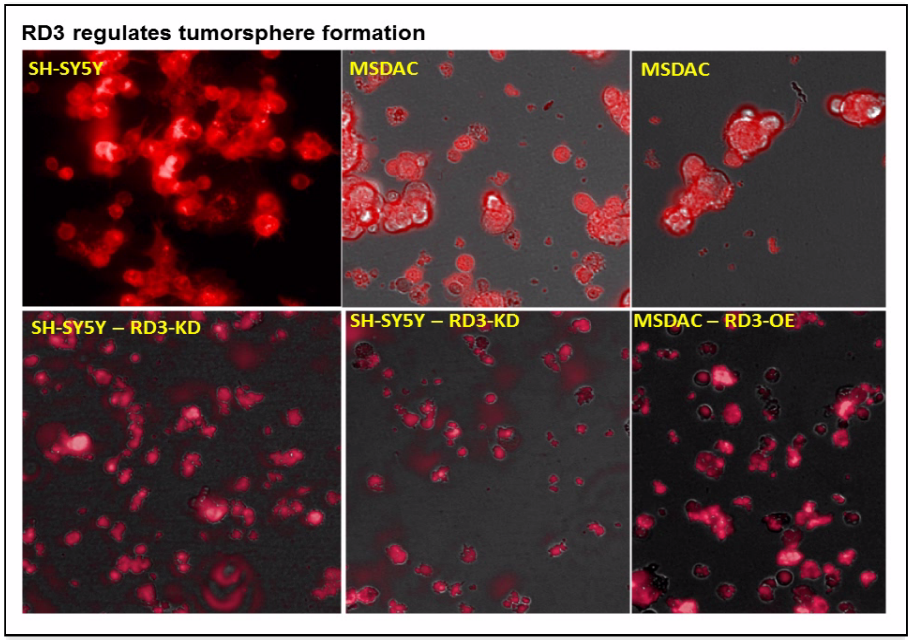


**Supplementary Video S1: *RD3 regulates* tumorosphere formation capacity.** Representative video clips from limiting dilution tumorosphere formation assay showing the influence of RD3 in the regulation of tumorosphere formation capacity. Serially diluted SH-SY5Y cells with and without RD3 silencing or MSDACs with and without RD3 re-expression plated in 96-well culture plates were stained with DiI, and were imaged in high-content real-time fluorescent imager, Operetta for every 20 min for period of 18 h. SH-SY5Y cells exhibited monolayer cell spreading without any organized tumorosphere formations (*Top left panel*). Silencing RD3 SH-SY5Y cells resulted in the formation of organized tumorospheres and defied any monolayer cell spreading (*Bottom left and middle panel*). MSDACs exhibited organized tumorosphere formation without any monolayer cell spreading (*Top right and middle panel*). Re-expressing RD3 in MSDACs completely abrogated organized tumorosphere formation (*Bottom left panel*).